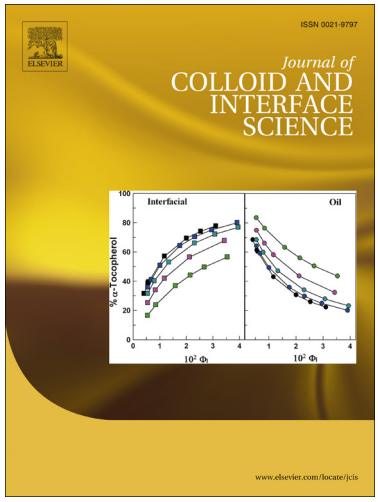

Glucose biosensor based on GOx/HRP bienzyme at liquid-crystal/aqueous interface

Mashooq Khan, Soo-Young Park

PII: S0021-9797(15)30027-8
DOI: http://dx.doi.org/10.1016/j.jcis.2015.07.010
Reference: YJCIS 20564

To appear in: *Journal of Colloid and Interface Science*

Received Date: 25 April 2015
Revised Date: 3 July 2015
Accepted Date: 6 July 2015

Please cite this article as: M. Khan, S-Y. Park, Glucose biosensor based on GOx/HRP bienzyme at liquid-crystal/aqueous interface, *Journal of Colloid and Interface Science* (2015), doi: http://dx.doi.org/10.1016/j.jcis.2015.07.010

Glucose biosensor based on GOx/HRP bienzyme at liquid-crystal/aqueous interface

Mashooq Khan and Soo-Young Park*

Department of Polymer Science and Engineering, School of Applied Chemical Engineering, #1370 Sangyuk-dong, Buk-gu, Daegu 702-701, Korea.

*Corresponding Author email: psy@knu.ac.kr

Abstract: Glucose oxidase (GOx) and horseradish peroxidase (HRP) were co-immobilized to the polyacrylicacid block of apoly(acrylicacid-*b*-4-cyanobiphenyl-4′-undecylacrylate) (PAA-*b*-LCP) copolymer in water. PAA-*b*-LCP was strongly anchored by the LCP block in 4-cyano-4′-pentylbiphenyl (5CB) which was contained in transmission electron microscope (TEM) grid for glucose detection. The optimal conditions for the performance of the TEM grid glucose biosensor were studied in terms of the activity and stability of the immobilized enzymes. Glucose in water was detected by the 5CB changing from a planar to a homeotropic orientation, as observed through a polarized optical microscope. The TEM biosensor detected glucose concentrations at ≥0.02 mM, with an optimal GOx/HRP molar ratio of 3/1. This glucose biosensor has characteristics of enzyme sensitivity and stability, reusability, the ease and selective glucose detection which may provide a new way of detecting glucose.

Keywords: Bienzyme, glucose, biosensor, glucose oxidase, peroxidase, liquid crystal

Introduction:

Many operational approaches have been explored in the application of enzyme-based biosensors for glucose analysis in individuals with diabetes, in foods, and in bioprocess products. All the studied techniques have relied on the use of one or more enzymes for converting glucose to electro-active products. A plethora of glucose biosensors have been developed in the past decades by immobilizing glucose oxidase (GOx) or GOx co-immobilized with a peroxidase (e.g., horseradish peroxidase (HRP)) on the materials, such as metal nanoparticles, conducting polymers, carbon nanotubes, nanorods, graphene, and polymer membranes [1-7]. The main advantage of the bienzyme (GOx/HRP) glucose biosensor is its enhanced sensitivity due to the catalytically linked enzymes[6]. Several detection methods, such as luminescence, spectroscopy, chromatography and amperometric analysis, have been used as glucose biosensors. Among them amperometric glucose biosensors have served as a valuable tools[8]. The glucose detection with a bienzyme GOx/HRP system is based on the GOx-catalyzed oxidation of glucose (equation 1), which produces gluconic acid and hydrogen peroxide (H_2O_2), followed by the HRP-catalyzed reduction of H_2O_2 [8]. Scheme 1a shows that the immobilized HRP^{+3} reduces the H_2O_2 to hydroxyl ion (OH^-) and oxidizes itself to the oxidized state of HRP^{+5}; +3 and +5 are the oxidation state of the resting and intermediate enzyme respectively. The OH^- can take the available protons (H^+) in the system to produce water. Then the HRP^{+5} revert to HRP^{+3} either directly by taking electrons from an electron source or through a reducing substrate (M, an electron mediator) by a mechanism involving two sequential single-electron steps. The first of those steps leads to the generation of a second enzyme intermediate with the oxidation state of +4 which is subsequently reduced to the native enzyme HRP^{+3} by a second molecule of reducing substrate. The oxidized substrate then consumes electrons from an electron source and recycles

[9]. In the absence of usual reducing substrates and electron sources, H_2O_2 can perform a dual role as both an oxidant in the formation of HRP^{+5} and a typical one-electron donor (reductant for peroxidase) which yields hydroperoxyle radical ($HO_2^{\bullet}$) and superoxide ion radical ($O_2^{\bullet-}$) as shown in scheme 1b [10]. The $O_2^{\bullet-}$ is a highly reactive intermediate and can readily react with H^+ to form $HO_2^{\bullet}$. The two $HO_2^{\bullet}$ forms H_2O_2 and molecular oxygen. In the following step, the H_2O_2 decomposes to OH^- in the presence of a reducing agent (e.g., HRP) and the reaction continues as more H_2O_2 and H^+ are available [11]. Thus, an efficient glucose biosensor which utilizes the activity of generated OH^- from the HRP-catalyzed reduction of H_2O_2 without the aid of an electron source or mediator can be designed.

$$\text{Glucose} + \text{GOx} \longrightarrow \text{Gluconic acid} + H_2O_2 \qquad \text{---------- (1)}$$

Liquid crystal (LC) materials, with their high birefringence and extreme sensitivity to surface interactions, are poised to play an important role in the development of biosensors. LCs have been explored for developing immunoassays that eliminate the need for sophisticated instruments, because of the enhanced optical appearance of changes made to the LCs by an enzymatic reaction. This enhanced optical appearance of the molecular change is due to the low interfacial energy (10^{-6}–10^{-3} J/m^2) of LC molecules at the LC/aqueous interface[12]. For example, changes in the optical appearance of 4-cyano-4′-pentylbiphenyl (5CB, a nematic LC at room temperature) have been utilized for the detection of surfactants[13], lipids[14], proteins[15], synthetic polymers[16-18], endotoxins[19], and simple electrolytes[20] by polarized optical microscopy (POM). Previous studies have revealed that the response of 5CB can be tuned to external stimuli by functionalizing it with polyelectrolytes and surfactants[21]. Moreover, when these surfactants or polymer contain pH-sensitive functional groups, the orientations of LCs become sensitive to the pH in the aqueous phase. For example a TEM-grid pH sensor was

developed by doping 5CB with 4-pentylbiphenyl-4′-carboxylic acid (PBA) to visualize the local pH changes from the enzymatic hydrolysis of penicillin G by surface immobilized penicillinase. They observed a homeotropic-to-planar orientational (H-P) transition by a very small change in pH from 7.0 to 6.9 [21]. In our previous study the 5CB in a TEM grid cell functionalized with a pH-responsive amphiphilic poly(acrylicacid-b-4-cynobiphenyl-4-oxyundecylacrylate) (PAA-*b*-LCP) (TEM_{PAA}) exhibited a fast and reversible homeotropic (dark)-to-planar (bright) orientation change in 5CB in response to the deprotonation and protonation of PAA chains caused by high and low pH of the solution respectively [16, 22]. Similarly a TEM_{PAA} with immobilized urease has been used for urea detection. A planar-to-homeotropic (P-H) orientation was observed in presence of urea due to the deprotonation of the PAA chains by OH^- ion produced from the urease-catalytic reaction of urea [23]. The GOx immobilized covalently on TEM_{PAA} showed enhanced glucose detection at the 5CB/aqueous interface[24]. The small amount of glucose in solution was detected through a H-P orientation change of the 5CB. This change was attributed to the generation of H^+ which protonate the PAA chains and caused planar orientation. However, a 2 M NaCl solution had to be used to obtain the required initial homeotropic orientation after the GOx immobilization, which may affect the long-term stability of the biosensor, making the construction of the biosensor cell difficult and non-reusable. Therefore, utilizing a OH^- ion from a GOx/HRP system a simple, stable, and reliable glucose biosensor can be develop without using salt solution at 5CB/aqueous interface.

In this study, a glucose biosensor was designed by coating the 5CB in a TEM grid with PAA brushes at the 5CB/aqueous interface, using amphiphilic poly(acrylicacid-*b*-4-cyanobiphenyl-4′-undecylacrylate) (PAA-*b*-LCP), followed by co-immobilization of GOx/HRP on the PAA chains. This bienzyme-based glucose LC biosensor does not need a salt solution for

inducing the reference homeotropic orientation. The glucose was detected by a planar-to-homeotropic (P–H) orientation change of the 5CB in the TEM grid. The ease of detection and the high stability, activity, and sensitivity of the enzymes make this system suitable as a convenient biosensor for glucose detection.

Experimental

Preparation of materials: Microscope glass slides (Paul Marienfeld GmbH &Co.KG, Germany) were cleaned using piranha solution (***Caution***: piranha solution is extremely corrosive and must be handled carefully), washed subsequently with distilled water, and dried under nitrogen. Copper TEM specimen grids (G75; grid hole width of 285 µm, pitch of 340 µm, bar width of 55 µm, size of 3.05 mm, and thickness of 18 µm) were purchased from Ted Pella, Inc. The 5CB (Tokyo Chemical Industry Co., Ltd. (TCI), 100%), phosphate-buffered saline (PBS) buffer (Samchun Chemicals), Citrate buffer was prepared from 0.1 M solutions of citric acid and sodium citrate in distilled water. The desired pH=7 was obtained by adding the sodium citrate solution dropwise to the citric acid solution. GOx (E.C. 1.1.3.4; from *Aspergillus niger* as a salt-free lyophilized powder with a specific activity of > 100 units/mg), HRP (E.C. 1.11.1.7; Type VI, salt-free lyophilized powder with a specific activity of 330 units/mg), D-(+)-glucose, *N*-(3-dimethylaminopropyl)-*N*-ethylcarbodiimide hydrochloride (EDC·HCl), *N*-hydroxysulfosuccinimide sodium salt (NHS), sodium chloride, trifluoroacetic acid (TFA, 99%), octadecyltrichlorosilane (OTS), methanol, dichloromethane (DCM), yeast extract (YE), ascorbic acid, and human hemoglobin (Sigma-Aldrich) were used as received. PAA-*b*-LCP was synthesized using a method reported previously[16, 24]. The molecular weights of the PAA and *b*-LCP moieties in PAA-*b*-LCP are 11K and 5K, respectively (the numbers represent the number-average molecular weight; for example, 11K is 11,000 g/mol), and the polydispersity index (M_w/M_n) is 1.14.

Formation of PAA-*b*-LCPmonolayer: The monolayer experiments were performed with a Langmuir–Blodgett (LB) KSV Layer builder (AAA100178; KSV Instruments Ltd., Finland) connected to a KSV minimicro trough, which was surrounded by an environmental chamber.

The working area of the trough was 17 × 5 cm^2. All the experiments were performed at room temperature. The surface pressure of the monolayer at the air/liquid interface was measured using a Wilhelmy plate attached to a microbalance. PAA-*b*-LCP was dissolved in dioxane and kept at 60°C for 2 days. Subsequently, toluene was added to the dioxane solution to obtain a final concentration of 1 mg/mL with a dioxane/toluene ratio of 6/4 (v/v). When a zero surface pressure was reached, 100 µL of the PAA-*b*-LCP solution was spread immediately on the water to form a monolayer. One hour after monolayer formation, the monolayer was compressed, expanded, and compressed again at a rate of 3 mm/min to achieve equilibrium. The areal density of the monolayer was controlled by maintaining the surface pressure on the spread LB film at 35mN/m (see Figure SI 1).

Device fabrication: The flow cell used in this study was prepared according to the method reported by Khan and Park[24]. Briefly, microscope glass slides were cleaned and coated with OTS to align the 5CB perpendicularly to the glass surface. A TEM grid was placed on the surface of the 12 × 8 mm^2 OTS-coated glass that was glued to another glass slide with epoxy. The 5CB (1µL) was dropped onto a TEM grid using a 5µL glass syringe (Hamilton Co., Reno, NV, USA). Excess 5CB was removed with a capillary tube in order to obtain a uniform thin layer of~18 µm thickness. To transfer the PAA-*b*-LCP monolayer onto the surface of the 5CB in the TEM grid, the 5CB-filled TEM grid was slowly inserted grid side down into the LB bath, coming to rest on a 2-mm-thick silicon spacer attached to a glass slide in the LB bath. The two glass slides spaced with silicon rubber were then clipped with binder clips. The internal volume of the flow cell was 0.4mL. The inlet and outlet ports for exchanging the solutions were syringe needles punched through the silicon rubber. Figure SI 2 shows the schematic diagram and actual photograph of the flow cell.

Immobilization of GOx/HRP: GOx and HRP were co-immobilized to the PAA chains on the TEM grid by using a method reported elsewhere[25]. Briefly, the PAA chains were activated with 0.4 M EDC·HCl and 0.1 M NHS for 1 h, after which 6mL of the GOx/HRP mixture was passed through the flow cell, which was then held for 12 h at room temperature. The fabricated TEM grid cell is denoted here after as $TEM_{PAA\text{-}GOx:HRP}$. To obtain the optimum ratio of the GOx and HRP, several GOx/HRP mixtures with a fixed concentration of HRP (12.5 μM) and different concentrations of GOx (12.50, 18.75, 25, 31.25, 37.5, 43.75, and 50 μM) were used for the immobilization.

Practical analysis: In order to test the $TEM_{PAA\text{-}GOx:HRP}$ for its ability to detect glucose in a sample, mixtures of YE (1 mg/mL), hemoglobin (5 mM), ascorbic acid (0.1 mM), and glucose (0.01, 0.05, 0.1, or 2 mM) were prepared. YE is the common name for various forms of the processed yeast products made by extracting the body cell contents, and is commonly used as food additives or flavorings and as nutrients for individuals with diabetes and high cholesterol[26]. YE was used for practical analysis because it contains all the ingredients of blood, such as saturated and unsaturated fats, sodium, potassium, magnesium, chromium, carbohydrate sugars, protein, and vitamin B complex, and may mimic the contents of a real blood sample upon the addition of hemoglobin, ascorbic acid, and glucose. Figure SI 3 shows the chromatograms obtained from the high-performance liquid chromatography (HPLC) of YE, glucose, and a YE/glucose mixture. The chromatogram of YE did not show a peak at retention time (RT) = 9.75 min for glucose, but that of the YE/glucose mixture exhibited a characteristic peak of glucose at RT = 9.75 min, confirming that the YE used did not contain any glucose and that the YE/glucose mixture could be used as a standard sample for demonstrating the practical analysis of the $TEM_{PAA\text{-}GOx:HRP}$ sensor.

Instrumentation: Images and videos of the TEM grid cells, taken under a polarized optical microscope (ANA-006; Leitz, Germany) with a crossed polarizer state, were recorded using a CCD camera (STC-TC83USB; Samwon, Korea). The HPLC analysis was carried out using an HPLC instrument (Model 600E; Waters Co.) with a column (Sugar-Pak I, 6.5×300mm) and a refractive index detector (RI, Model 410). Ca-EDTA buffer (50mg Ca-EDTA/1L dH_2O) was used as the mobile phase, with a column flow rate of 0.5 mL/min at 90°C. The birefringence (Δn) was measured using a tilting compensator (2073 K, equipped with a calcite compensator plate; Leitz, Germany) with the source light intensity at 50% of full illumination. At the zero position of the compensator, the crystal axis was parallel to the polarizer axis. The Δn is defined as Γ/d, where Γ is the phase difference and d is the sample thickness (18000 nm). The Γ value was measured from the tilting angle (2i) using the equation $\Gamma = 10^4 f(2i) \times \frac{C}{10^4}$, where f(2i) is tabulated in the instrument manual and C is the compensator constant (4.54×10^4). The measurements were made in triplicate, and the error bar represents the standard deviation.

Results and Discussion:

Characteristics of $TEM_{PAA\text{-}GOx:HRP}$ grid cell: Figure 1a shows a POM image of the $TEM_{PAA\text{-}GOx:HRP}$, exhibiting a typical planar orientation under crossed polarizers at pH 7. The TEM grid cell with only the PAA-*b*-LCP coating (TEM_{PAA}) showed a planar orientation, as reported elsewhere[24]. This orientation was maintained after the immobilization of enzymes on the coating. A planar-to-homeotropic (P–H) change occurred with the time pass (t_{pass}) of ~15 min, when the aqueous medium in the TEM grid was replaced with a 25 mM glucose solution, as shown in Figure 1b. This change in the 5CB orientation might be the result of the GOx-catalyzed oxidation of glucose, followed by the reduction of H_2O_2 by HRP, which generates OH^- at the 5CB/aqueous interface. These OH^- could take H^+ lead to the deprotonation of the carboxylic groups in the PAA chains, generating a high density of negative charges that may form an electric field. Because 5CB is a negative dielectric anisotropic material that favors homeotropic orientation in the presence of an electric field, P–H change results. When $TEM_{PAA\text{-}GOx}$ (without HRP immobilization) was subjected to the same concentration of glucose, no P–H change was observed (Figure 1c). Similarly, when $TEM_{PAA\text{-}HRP}$ (without GOx immobilization) was subjected to the same concentration of glucose, no P–H change was observed (Figure 1d). These results suggest that the OH^- generated at the 5CB/aqueous interface were responsible for altering the 5CB orientation. To confirm that electrons generated by the HRP-catalyzed H_2O_2 reduction caused a P–H change of 5CB in the TEM grid, additional experiments were performed with the addition of a H_2O_2 solution, as shown in Figure SI 4. The P–H change was observed when $TEM_{PAA\text{-}HRP}$ was subjected to a 20 mM H_2O_2 solution (Figure SI 4a), but no P–H change was observed when glucose was injected into the $TEM_{PAA\text{-}HRP}$ (Figure 1d). A 20 mM H_2O_2 solution was also injected into the enzyme-free TEM_{PAA} in order to check whether H_2O_2 itself can cause a

homeotropic orientation of 5CB. The initial planar orientation was retained (Figure SI 4b), indicating that the P–H change was caused by the HRP-catalyzed H_2O_2 reduction at the 5CB/aqueous interface. Previous studies have shown that 5CB coated with polyelectrolytes (PEs) at the LC/aqueous interface exhibits homeotropic orientation due to an increase in the charged density by the PE. For example, 5CB coated with strong PE brushes such as poly(styrenesulfonate) and quarternized poly(4-vinylpyridine) at the LC/aqueous interface had a homeotropic orientation due to the charged state of the polymer at any pH [27-28]. A P–H orientation change of 5CB was also observed when a TEM_{PAA} biosensor with urease immobilized on the PAA chains was subjected to an aqueous urea solution [23]. This change was attributed to the hydroxyl ions that were generated during the urease-catalyzed reaction of urea, which deprotonated the PAA chains, leading to the homeotropic orientation by increasing the charged density on the 5CB/aqueous interface. Thus, it can be concluded that the P–H orientation change of $TEM_{PAA\text{-}GOx:HRP}$ in the glucose solution was due to the GOx/HRP reaction generating a high charge density at the 5CB/aqueous interface.

Choice of buffer system: Protons generated from the dissociation of gluconic acid (one of the major products in the GOx-catalyzed oxidation of glucose) can protonate the PAA chains on the 5CB/aqueous interface and cause interference during glucose detection. In order to prevent such interference from occurring, buffer solutions were used for maintaining the pH of the medium. PBS and citrate buffers were tested with the $TEM_{PAA\text{-}GOx:HRP}$ biosensor, in terms of enzyme activity and stability for glucose detection. These two buffer solutions are commonly used in biological tests. Figure 2 shows POM images of $TEM_{PAA\text{-}GOx:HRP}$ in PBS and citrate buffers with injection of a 25 mM glucose solution after a certain time in days (t_{pass}). A clear P–H orientation change was observed in both buffers with the 25 mM glucose solution injected at t_{pass} = 20 days.

At t_{pass}=25 and 30 days, the homeotropic orientation in the citrate buffer had deteriorated, creating some patches (Figure 2b), whereas a clear homeotropic orientation was observed throughout the time passes in the PBS buffer (Figure 2a). This suggests that PBS buffer allows longer stability of the GOx/HRP enzymes on the PAA chains than does citrate buffer. Therefore, PBS buffer was used for all the following experiments, unless otherwise specified.

Optimization of GOx/HRP ratio: Since GOx and HRP play different roles in glucose detection, the ratio of these two enzymes on the PAA chains may influence the overall performance of the biosensor at a test pH of 7. The amount of GOx was varied to find the optimum ratio for immobilization of GOx with a fixed concentration of HRP. Figure 3a shows the POM images (under crossed polarizers) of $TEM_{PAA\text{-}GOx:HRP}$ at different GOx/HRP (G/H) ratios in a 25 mM glucose solution at t_{pass}=3 min. No significant P–H change was observed at G/H=1 (Figure 3ai). Darkness in the image appeared at G/H=2 (Figure 3aii), and became uniform and apparent at G/H = 2.5, 3, and 3.5 (Figures 3aiii–v), indicating that complete homeotropic orientation was obtained. However, the black image became less apparent at G/H = 4 (Figure avi), suggesting that the optimum GOx/HRP ratio is 3 for glucose detection. Figure 3b shows the time required for a complete P–H change as a function of G/H in a 25 mM glucose solution. The shortest time (<50 s) was observed at G/H = ~3. This result also indicates that the highest activity of the GOx/HRP on the PAA chains is at a G/H ratio of ~3. Therefore, the G/H ratio of 3 was used for the subsequent experiments.

Sensitivity of $TEM_{PAA\text{-}GOx:HRP}$ biosensor: Figure 4a shows the POM images of $TEM_{PAA\text{-}GOx:HRP}$ at different glucose concentrations (C_0) under crossed polarizers. The reference planar orientation was preserved at C_0=0.01 mM (Figure 4ai). Slight darkness appeared at C_0=0.02 mM (Figure 4aii), the dark zone increased until C_0 = 0.5 mM (Figures 4aiii–vi), and a completely dark

image from P–H change was observed at $C_0 \geq 1$ mM (Figures 4av–x). Thus, the $TEM_{PAA\text{-}GOx:HRP}$ biosensor could detect glucose at $C_0 \geq 0.02$ mM. The difference in the optical appearance with increasing C_0 can be an indication of the glucose level in the medium. This optical appearance is due to the in-plane birefringence of the LC molecules, and therefore the precise measurement of Δn is important for the quantitative analysis of glucose. Figure 4b shows the Δn change as a function of C_0. The Δn value decreased linearly until C_0 = 0.75mM and then slowly decreased until C_0 = 2 mM, finally reaching saturation at Δn = ~0.02. The visible detection range of the $TEM_{PAA\text{-}GOx:HRP}$ biosensor may allow the glucose detection with naked eyes using a POM. Figure 4c shows the POM images of $TEM_{PAA\text{-}GOx:HRP}$ on sequential exposure to PBS buffer of pH=8.5-7.2 after glucose detection. The initial homeotropic orientation retains at pH=8.5 and 8 (Figure 4ai and ii). A slight H-P change is observed at pH=7.8 (Figure 4aiii). The planar orientation become more visible at pH=7.6 and 7.4 (4aiv and v) and is saturated at pH=7.2 as shown in Figure 4avi. Dong et al., demonstrated the dissociation behavior of PAA brushes at the gold surface. They found that the COOH gradually started to deprotonate at pH ≥ 6.5 to COO^- reach a maximum deprotonation at pH=9 [29]. Thus the difference in the birefringence may be due to the varying charged density on the PAA chains at different pHs.

Reuse of $TEM_{PAA\text{-}GOx:HRP}$: Reusability is one of the important characteristics for a biosensor. The $TEM_{PAA\text{-}GOx:HRP}$ biosensor reusability was tested by alternately exposing it to first a glucose solution and then PBS buffer (pH=7). Figure 5 shows the Δn values of $TEM_{PAA\text{-}GOx:HRP}$ as a function of the cycle of the sequential exposures to a 0.5 mM glucose solution, PBS buffer, a 1 mM glucose solution, and PBS buffer. The reason why different concentrations of glucose solution were used was to check whether the sensitivity with respect to glucose concentration was maintained after washing with PBS. In each cycle, the Δn value was found to be

0.079±0.0008 after washing, and lowered to 0.028 ± 0.0005 and 0.042 ± 0.0003 after exposure to the 1 and 0.5 mM glucose solutions, respectively. This result indicates that the $TEM_{PAA\text{-}GOx:HRP}$ biosensor can be used for multiple detections, even at different glucose concentrations. In our previous study, the TEM sensor controlled with 2 M NaCl could be utilized only once for glucose detection because of the difficulty in re-obtaining the reference homeotropic orientation of the 5CB. Thus, this $TEM_{PAA\text{-}GOx:HRP}$ has a lot of merits for a biosensor.

Practical evaluation: Figure 6 shows the POM images (under crossed polarizers) of the $TEM_{PAA\text{-}GOx:HRP}$ after injection of YE/glucose mixture solutions of different glucose concentrations. The initial planar orientation was maintained with the pure YE and the mixture containing 0.01 mM glucose (Figures 6a and b). However, slight homeotropic orientations were observed with the mixtures containing 0.05 or 0.1 mM glucose (Figures 6c and d), and the homeotropic orientation became more visible with the mixture containing 2 mM glucose (Figure 6e). The Δn values obtained from the mixtures containing 0.05 and 0.1 mM glucose (Figures 6c and d) were 0.073 ± 0.0005 and 0.069 ± 0.0008, respectively. These Δn values were similar to those obtained from the pure glucose solution at C_0 = 0.05 and 0.1 mM (Figures 4c and e), indicating that the glucose in the YE/glucose mixtures can be independently and quantitatively detected with the $TEM_{mixed\text{-}GOx}$ without interference from YE.

Conclusion: A GOx/HRP bienzyme system for glucose detection at the 5CB/aqueous interface was demonstrated. The optimal GOx/HRP ratio (3/1) enabled glucose detection in the medium at concentrations ≥ 0.02 mM, by observation of the P–H orientation change of 5CB using POM. The high enzyme sensitivity and stability, its reusability, and the selective glucose detection in a complex mixture of this TEM grid glucose biosensor may provide a new method for the detection of glucose.

Acknowledgment: This work was supported by the National Research Foundation of Korea (NRF-2011-0020264) and (NRF-2014R1A2A1A11050451).

References

[1] X. Chu, D. Duan, G. Shen, R. Yu, Amperometric glucose biosensor based on electrodeposition of platinum nanoparticles onto covalently immobilized carbon nanotube electrode, Talanta, 71 (2007) 2040-2047.
[2] M.-L. Ho, J.-C. Wang, T.-Y. Wang, C.-Y. Lin, J.F. Zhu, Y.-A. Chen, T.-C. Chen, The construction of glucose biosensor based on crystalline iridium(III)-containing coordination polymers with fiber-optic detection, Sensors and Actuators B: Chemical, 190 (2014) 479-485.
[3] K.-Y. Hwa, B. Subramani, Synthesis of zinc oxide nanoparticles on graphene–carbon nanotube hybrid for glucose biosensor applications, Biosensors and Bioelectronics, 62 (2014) 127-133.
[4] X. Jing-Juan, C. Hong-Yuan, Amperometric Glucose Sensor Based on Coimmobilization of Glucose Oxidase and Poly(p-phenylenediamine) at a Platinum Microdisk Electrode, Anal. Biochem., 280 (2000) 221-226.
[5] G. Liu, Y. Lin, Amperometric glucose biosensor based on self-assembling glucose oxidase on carbon nanotubes, Electrochem. Commun., 8 (2006) 251-256.
[6] M. Gu, J. Wang, Y. Tu, J. Di, Fabrication of reagentless glucose biosensors: A comparison of mono-enzyme GOD and bienzyme GOD–HRP systems, Sensors and Actuators B: Chemical, 148 (2010) 486-491.
[7] J. Lu, I. Do, L.T. Drzal, R.M. Worden, I. Lee, Nanometal-Decorated Exfoliated Graphite Nanoplatelet Based Glucose Biosensors with High Sensitivity and Fast Response, ACS nano, 2 (2008) 1825-1832.
[8] J. Wang, Electrochemical Glucose Biosensors, Chemical Reviews, 108 (2008) 814-825.
[9] A.J.S. Ahammad, Hydrogen Peroxide Biosensors Based on Horseradish Peroxidase and Hemoglobin, J Biosens Bioelectron, S9 (2013) 1-11.
[10] J. Hernández-Ruiz, M.B. Arnao, A.N. Hiner, F. García-Cánovas, M. Acosta, Catalase-like activity of horseradish peroxidase: relationship to enzyme inactivation by H2O2, Biochemical Journal, 354 (2001) 107-114.
[11] P. Praus, J. Matys, O. Kozák, Photocatalytic decomposition of phenol by nanocomposite of ZnS nanoparticles and montmorillonite, Journal of the Brazilian Chemical Society, 23 (2012) 1900-1906.
[12] S.J. Woltman, G.D. Jay, G.P. Crawford, Liquid crystal material find a new order in biomedical application, Nature Material, 6 (2007) 929-938.
[13] J.M. Brake, A.D. Mezera, N.L. Abbott, Effect of Surfactant Structure on the Orientation of Liquid Crystals at Aqueous-Liquid Crystal Interfaces, Langmuir, 19 (2003) 6436-6442.
[14] J.M. Brake, M.K. Daschner, Y.Y. Luk, N.L. Abbott, Biomolecular Interactions at Phospholipid-Decorated Surfaces of Liquid Crystals, SCIENCE, 302 (2003) 2094-2097.
[15] V.K. Gupta, J.J. Skaife, T.B. Dubrovsky, N.L. Abbott, Optical Amplification of Ligand-Receptor Binding Using Liquid Crystals, SCIENCE, 279 (1998) 2077-2080.
[16] D.Y. Lee, J.M. Seo, W. Khan, J.A. Kornfield, Z. Kurjib, S.Y. Park, pH-responsive aqueous/LC interfaces using SGLCP-b-polyacrylic acid block copolymers, Soft Matter, 6 (2010) 1964-1970.
[17] M. Omer, M. Khan, Y.K. Kim, J.H. Lee, I.-K. Kang, S.-Y. Park, Biosensor utilizing a liquid crystal/water interface functionalized with poly(4-cyanobiphenyl-4′-oxyundecylacrylate-b-((2-dimethyl amino) ethyl methacrylate)), Colloids and Surfaces B: Biointerfaces, 121 (2014) 400-408.
[18] M.-V. Meli, I.H. Lin, N.L. Abbott, Preparation of Microscopic and Planar Oil−Water Interfaces That Are Decorated with Prescribed Densities of Insoluble Amphiphiles, Journal of the American Chemical Society, 130 (2008) 4326-4333.
[19] D.S. Miller, N.L. Abbott, Influence of droplet size, pH and ionic strength on endotoxin-triggered ordering transitions in liquid crystalline droplet, Soft Matter, 9 (2013) 374-382.
[20] R.J. Carlton, J.K. Gupta, C.L. Swift, N.L. Abbott, Influence of simple electrolytes on the orientational ordering of thermotropic liquid crystals at aqueous interfaces, Langmuir, 28 (2012) 31-36.

[21] X. Bi, D. Hartono, K.-L. Yang, Real-Time Liquid Crystal pH Sensor for Monitoring Enzymatic Activities of Penicillinase, Adv. Func. Mater., 19 (2009) 3760-3765.
[22] J.M. Seo, W. Khan, S.-Y. Park, Protein detection using aqueous/LC interfaces decorated with a novel polyacrylic acid block liquid crystalline polymer, Soft Matter, 8 (2012) 198-203.
[23] M. Khan, Y. Kim, J.H. Lee, I.-K. Kang, S.-Y. Park, Real-time liquid crystal-based biosensor for urea detection, Analytical Methods, 6 (2014) 5753-5759.
[24] M. Khan, S.-Y. Park, Liquid Crystal-Based Proton Sensitive Glucose Biosensor, Analytical Chemistry, 86 (2013) 1493-1501.
[25] G.C.M. Steffens, L. Nothdurft, G. Buse, H. Thissen, H.H. ocker, D. Klee, High density binding of proteins and peptides to poly(d,l-lactide) grafted with polyacrylic acid, Biomaterials, 23 (2002) 3523-3531.
[26] R. Anderson, Elevated intake of supplemental chromium improved glucose and insulin variables in individuals with type 2 diabetes, Diabetes, 46 (1997) 1786-1791.
[27] M. Omer, M. Islam, M. Khan, Y. Kim, J. Lee, I.-K. Kang, S.-Y. Park, Liquid crystal-based biosensors using a strong polyelectrolyte-containing block copolymer, poly(4-cyanobiphenyl-4′-oxyundecylacrylate)-b-poly(sodium styrene sulfonate), Macromol. Res., 22 (2014) 888-894.
[28] M. Omer, S.-Y. Park, Preparation of QP4VP-b-LCP liquid crystal block copolymer and its application as a biosensor, Anal Bioanal Chem, (2014) 1-10.
[29] R. Dong, M. Lindau, C.K. Ober, Dissociation Behavior of Weak Polyelectrolyte Brushes on a Planar Surface, Langmuir, 25 (2009) 4774-4779.

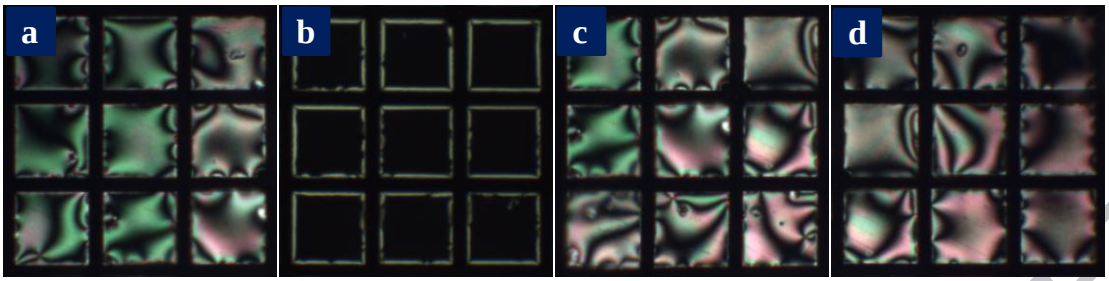

Figure 1. Polarized optical microscopy images of (a) $TEM_{PAA\text{-}GOx:HRP}$ before the injection of glucose, and (b) $TEM_{PAA\text{-}GOx:HRP}$, (c) $TEM_{PAA\text{-}GOx}$, and (d) $TEM_{PAA\text{-}HRP}$ after the injection of a 25mM aqueous glucose solution. $TEM_{PAA\text{-}GOx:HRP}$, fabricated transmission electronic microscopy grid cell with glucose oxidase and horseradish peroxidase co-immobilized to the polyacrylic acid block of poly(acrylicacid-*b*-4-cynobiphenyl-4′-undecylacrylate); $TEM_{PAA\text{-}GOx}$, fabricated grid cell with only glucose oxidase immobilized; $TEM_{PAA\text{-}HRP}$, fabricated grid cell with only horseradish peroxidase immobilized.

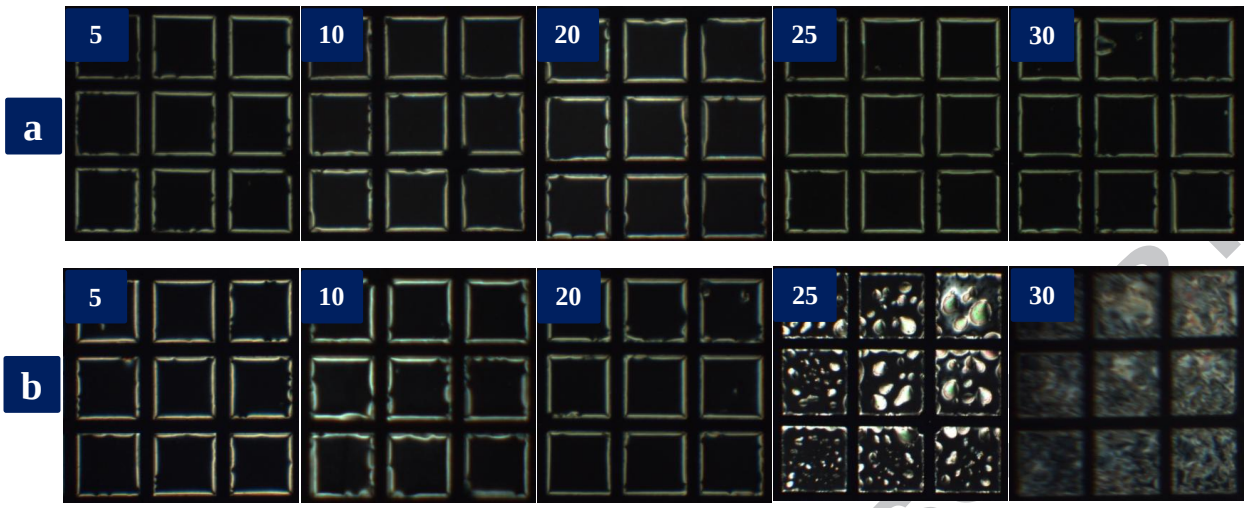

Figure 2. Polarized optical microscopy images of $TEM_{PAA\text{-}GOx:HRP}$ in (a) phosphate-buffered saline and (b) citrate buffers after injection of a 25 mM glucose solution at t_{pass} (in days). The numeral in the inset represents the number of days. $TEM_{PAA\text{-}GOx:HRP}$, fabricated transmission electronic microscopy grid cell with glucose oxidase and horseradish peroxidase co-immobilized to the polyacrylic acid block of poly(acrylicacid-*b*-4-cynobiphenyl-4′-undecylacrylate).

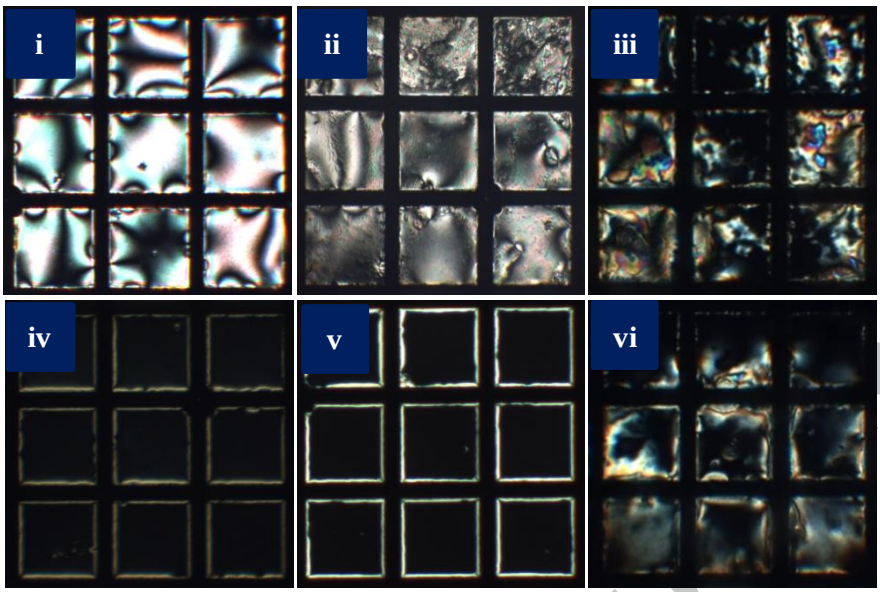

(a)

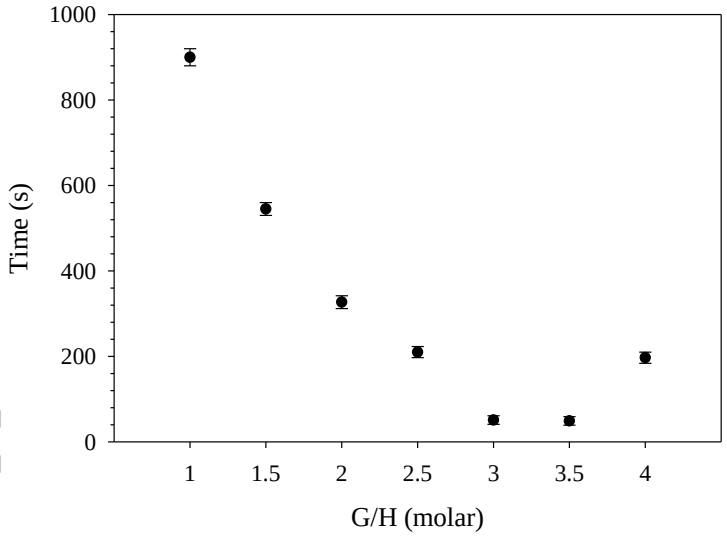

(b)

Figure 3. (a) Polarized optical microscopy images (under crossed polarizers) of the $TEM_{PAA\text{-}GOx:HRP}$ cell at the glucose oxidase/horseradish peroxidase (G/H) ratios of (i) 1, (ii) 2, (iii) 2.5, (iv) 3, (v) 3.5, and (iv) 4, in a 25 mM glucose solution. (b) The time required for a complete planar-to-homeotropic change as a function of G/H ratio in a 25 mM glucose solution. $TEM_{PAA\text{-}GOx:HRP}$, fabricated transmission electronic microscopy grid cell with glucose oxidase and horseradish peroxidase co-immobilized to the polyacrylic acid block of poly(acrylicacid-*b*-4-cynobiphenyl-4′-undecylacrylate).

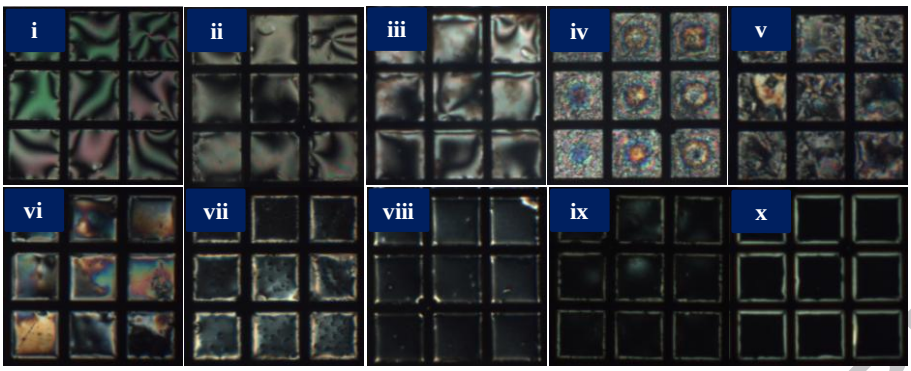

(a)

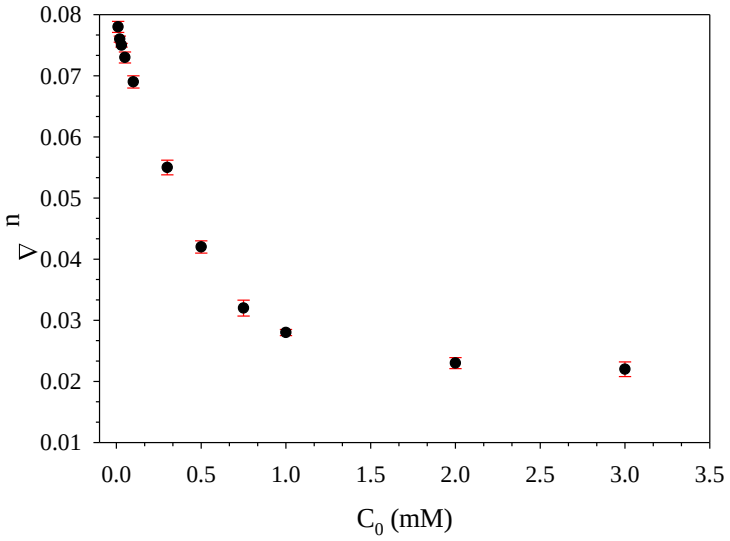

(b)

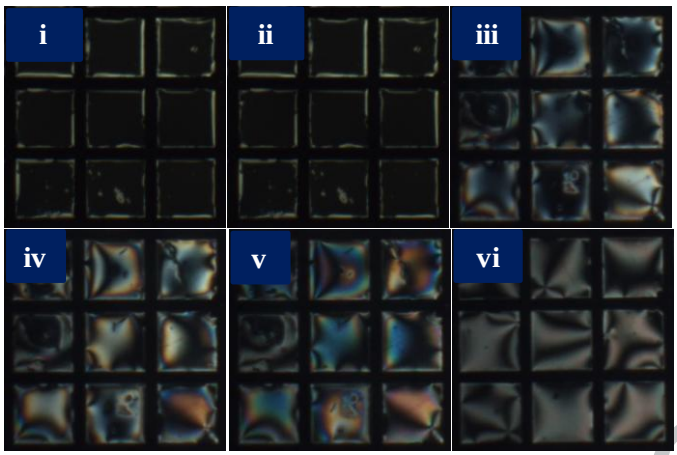

(c)

Figure 4. (a) Polarized optical microscopy (POM) images (under crossed polarizers) of $TEM_{PAA\text{-}GOx\text{-}HRP}$ in a glucose solution at concentration (C_0) values of (i) 0.01, (ii) 0.02, (iii) 0.05, (iv) 0.075, (v) 0.1, (vi) 0.3, (vii) 0.5, (viii) 0.75, (ix) 1, and (x) 10 mM. (b) A plot of the birefringence (Δn) measured from the POM images in (a) as a function of C_0. (c) $TEM_{PAA\text{-}GOx:HRP}$ in PBS buffer at pH=(i) 8.5, (ii) 8, (iii) 7.8, (iv) 7.6, (v) 7.4, and (vi) 7.2 after glucose detection. $TEM_{PAA\text{-}GOx:HRP}$, fabricated transmission electronic microscopy grid cell with glucose oxidase and horseradish peroxidase co-immobilized to the polyacrylic acid block of poly(acrylicacid-*b*-4-cynobiphenyl-4′-undecylacrylate).

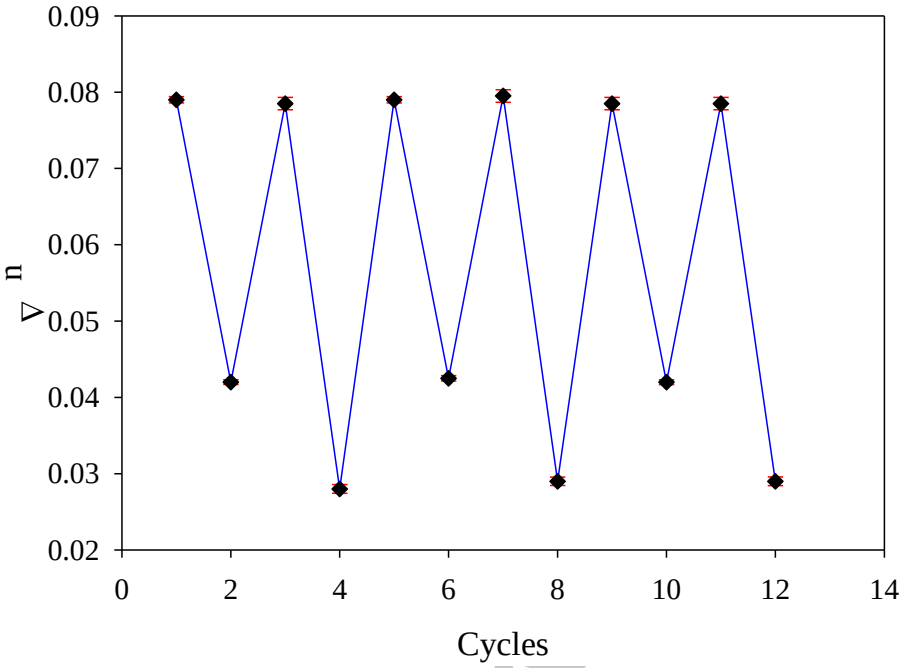

Figure 5. Birefringence (Δn) value of the $TEM_{PAA\text{-}GOx:HRP}$ sensor with three cycles of sequential exposure to a 0.5 mM glucose solution, PBS buffer, a 1 mM glucose solution, and PBS buffer. $TEM_{PAA\text{-}GOx:HRP}$, fabricated transmission electronic microscopy grid cell with glucose oxidase and horseradish peroxidase co-immobilized to the polyacrylic acid block of poly(acrylicacid-*b*-4-cynobiphenyl-4′-undecylacrylate).

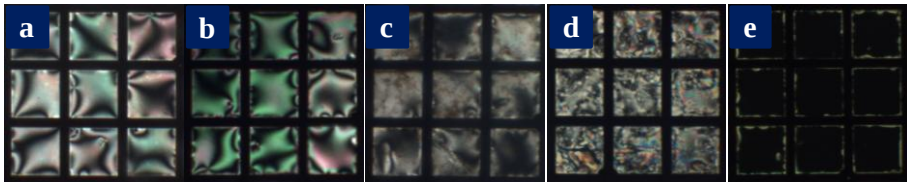

Figure 6. Polarized optical microscopy images of the $TEM_{PAA\text{-}GOx:HRP}$ grid cell after injection of a yeast extract/glucose mixture containing glucose concentrations of (a) 0, (b) 0.01, (c) 0.05, (d) 0.1, and (e) 2 mM. $TEM_{PAA\text{-}GOx:HRP}$, fabricated transmission electronic microscopy grid cell with glucose oxidase and horseradish peroxidase co-immobilized to the polyacrylic acid block of poly(acrylicacid-*b*-4-cynobiphenyl-4′-undecylacrylate).

$$H_2O_2 + HRP^{+3} \longrightarrow HRP^{+5} + 2OH^-$$
$$2OH^- + 2H^+ \longrightarrow 2H_2O$$
$$HRP^{+5} + M \longrightarrow HRP^{+4} + M^{+1}$$
$$HRP^{+4} + M \longrightarrow HRP^{+3} + M^{+1}$$
$$2M^{+1} + 2e^- \longrightarrow 2M$$

(a)

$$H_2O_2 + HRP^{+3} \longrightarrow HRP^{+5} + 2OH^-$$
$$2OH^- + 2H^+ \longrightarrow 2H_2O$$
$$HRP^{+5} + 2H_2O \longrightarrow HRP^{+3} + HO_2^{\cdot} + O_2^{\cdot -}$$
$$O_2^{\cdot -} + H^+ \rightleftharpoons HO_2^{\cdot}$$
$$H_2O_2 + HRP^{+3} \longrightarrow HRP^{+5} + 2OH$$

(b)

Scheme 1. HRP-catalyzed reduction of H_2O_2 in available H^+ (a) with an electron mediator (M) and an electron source, and (b) without an electron mediator.

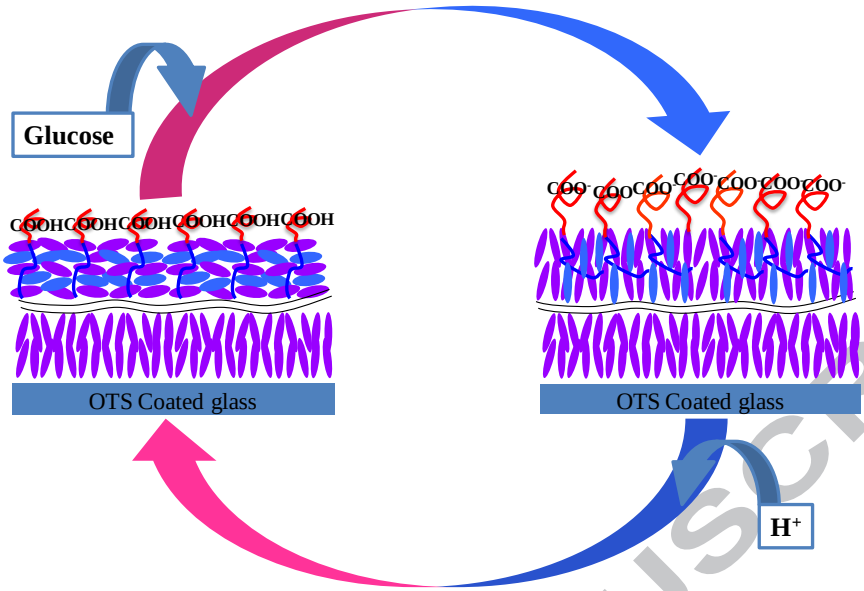

Figure. Table of contents (TOC) image.